Journal of the Korean Crystal Growth and Crystal Technology
Vol. 23, No. 1 (2013) 20-26
http://dx.doi.org/10.6111/JKCGCT.2013.23.1.020

Effects of convection on physical vapor transport of Hg_2Cl_2 in the presence of Kr - Part I: under microgravity environments

Yong Keun Lee and Geug-Tae Kim*,†

Graduate School of NID Fusion Technology, Seoul National University of Science and Technology, Seoul 139-743, Korea
**Department of Nano-Bio Chemical Engineering, Hannam University, Taejon 305-811, Korea*

(Received November 29, 2012)
(Revised January 2, 2013)
(Accepted January 18, 2013)

Abstract Special attention in the role of convection in vapor crystal growth has been paid since some single crystals under microgravity environments less than 1 g_0 exhibits a diffusive-convection mode and much uniformity in front of the crystal regions than a normal gravity acceleration of 1 g_0. The total molar fluxes show asymmetrical patterns in interfacial distribution, which indicates the occurrence of either one single or more than one convective cell. As the gravitational level decreases form 1 g_0 down to 1.0×10^{-4} g_0, the intensity of convection, indicative of the maximum molar fluxes, is reduced significantly for $\Delta T = 30$ K and 90 K. The total molar fluxes decay first order exponentially with the partial pressure of component B, PB (Torr) for $20 \text{ Torr} \le P_B \le 300$ Torr, and two gravity accelerations of $g_y = 1$ g_0 and 0.1 g_0.

Key words Mercurous chloride, Convection, Microgravity

1. Introduction

Physical vapor transport (PVT) has become an important crystal growth process for a variety of acousto-optic materials. Of particular importance is the use of PVT for materials processing experiments in high gravity environments, which would provide a better and thorough understanding of transport phenomena occurring in the vapor phase and crystal growth phenomena. Until now many theoretical studies and quantitative experiments on transport phenomena in PVT have been extensively investigated. Most important theoretical works were achieved by Rosenberger et al. [1-6] and, recently extended for transition to chaos flow fields in specialty materials of mercurous chloride in applications of microgravity experiments by Duval [7-12]. They have addressed the underlying phenomena in the PVT processes on the relative importance and influencing parameters of diffusion-advection, thermal and/or solutal convection on mass transport. Our recent studies [13-17] are for PVT processes of specialty materials such as mercurous halides under normal and microgravity environments to investigate the role of convection on the mass transport rate and its transition from diffusion-dominated to circulatory convection-dominated regimes in relation to total pressure, temperatures of source and crystal ends, aspect ratio (transport length-to-width), wall temperature profiles, molecular weights.

It is the purpose of this paper to study the essence of convection covering the various gravity accelerations in the PVT processes of Hg_2Cl_2 crystal growth system. For this theoretical analysis of the PVT processes, a two-dimensional model is in horizontally oriented, cylindrical, closed ampoules in a two-zone furnace system. A mixture of Hg_2Cl_2 vapor and impurity of Krypton (Kr) will be considered under microgravity environments.

2. The Model

Mercurous chloride (Hg_2Cl_2) materials are important for applications in acousto-optic and opto-electronic devices such as Bragg cells, X-ray detectors operating at ambient temperature [11]. The equimolar Hg_2Cl_2 compound decomposes to two liquids at a temperature near 525°C where the vapor pressure is above 20 atm [18]. Because of this decomposition and high vapor pressure, Hg_2Cl_2 cannot be solidified as a single crystal directly from the stoichiometric melt. However, very similar to the mercurous bromide [19], mercurous chloride exhibits sufficiently high vapor pressure at low temperatures so that these crystals are usually grown by the physical vapor transport (PVT) in closed silica glass ampoules.

Consider a rectangular enclosure of height H and transport length L, shown in Fig. 1. The source is main-

†Corresponding author
Tel: +82-42-629-8837
Fax: +82-42-629-8835
E-mail: gtkim@hnu.kr

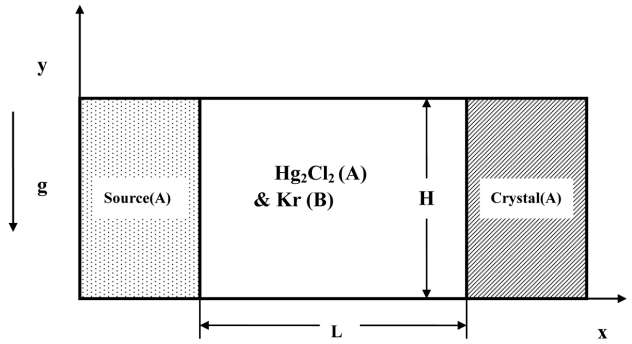

Fig. 1. Schematic and coordinates for a PVT crystal growth reactor of Hg_2Cl_2-Kr in a two-dimensional rectangular system.

tained at a temperature T_s, while the growing crystal is at a temperature T_c, with $T_s > T_c$. PVT of the transported component A (Hg_2Cl_2) occurs inevitably, due to presence of impurities, with the presence of a component B (Kr). The interfaces are assumed to be flat for simplicity. The finite normal velocities at the interfaces can be expressed by Stefan flow deduced from the one-dimensional diffusion-limited model [20], which would provide the coupling between the fluid dynamics and species calculations. On the other hand, the tangential component of the mass average velocity of the vapor at the interfaces vanishes. Thermodynamic equilibria are assumed at the interfaces so that the mass fractions at the interfaces are kept constant at $\omega_{A,s}$ and $\omega_{A,c}$. On the vertical non-reacting walls appropriate velocity boundary conditions are no-slip, the normal concentration gradients are zero, and wall temperatures are imposed as nonlinear temperature gradients. The density is assumed to be a function of both temperature and concentration. The ideal gas law and Dalton's law of partial pressures are used. The transport of fluid within a rectangular PVT crystal growth reactor is governed by a system of elliptic, coupled conservation equations for mass (continuity), momentum, energy and species (diffusion) can be represented by the generic equations, Eq. (1) through (4) [21] with their appropriate boundary conditions, Eq. (5) through (7). Let u_x, u_y denote the velocity components along the x- and y-coordinates in the x, y rectangular coordinate, and let T, ω_A, p denote the temperature, mass fraction of species A (Hg_2Cl_2) and pressure, respectively, where the superscript of * denotes the dimensionless [13-17]. The linear temperature profiles at wall boundary conditions only are considered.

$$\nabla^* \bullet \vec{\nabla}^* = 0, \tag{1}$$

$$\vec{\nabla}^* \bullet \nabla^* \vec{\nabla}^* = -\nabla^* p^* + Pr \cdot Ar \nabla^{*2} \vec{\nabla}^* - \frac{Ra \cdot Pr}{Ar} \cdot T^* \cdot e_g, \tag{2}$$

$$\vec{\nabla}^* \bullet \nabla^* T^* = Ar \nabla^{*2} T^* \tag{3}$$

$$\vec{\nabla}^* \bullet \nabla^* \omega_A^* = \frac{Ar}{Le} \nabla^{*2} \omega_A^* \tag{4}$$

On the walls ($0 < x^* < L/H$, $y^* = 0$ and 1):

$$u^*(x^*, 0) = u^*(x^*, 1) = v^*(x^*, 0) = v^*(x^*, 1) = 0 \tag{5}$$

$$\frac{\partial \omega_A^*(x^*,0)}{\partial y^*} = \frac{\partial \omega_A^*(x^*,1)}{\partial y^*} = 0,$$

$$T^*(x^*,0) = T^*(x^*,1) = \frac{T - T_c}{T_s - T_c}$$

On the source ($x^* = 0$, $0 < y^* < 1$):

$$u^*(0,y^*) = -\frac{1}{Le}\frac{\Delta\omega}{(1-\omega_{A,s})}\frac{\partial \omega_A^*(0,y^*)}{\partial x^*}, \tag{6}$$

$$v^*(0, y^*) = 0,$$

$$T^*(0, y^*) = 1,$$

$$\omega_A^*(0, y^*) = 1.$$

On the crystal ($x^* = L/H$, $0 < y^* < 1$):

$$u^*(L/H,y^*) = -\frac{1}{Le}\frac{\Delta\omega}{(1-\omega_{A,c})}\frac{\partial \omega_A^*(L/H,y^*)}{\partial x^*}, \tag{7}$$

$$v^*(L/H, y^*) = 0,$$

$$T^*(L/H, y^*) = 0,$$

$$\omega_A^*(L/H, y^*) = 0.$$

The vapor pressure [10] p_A of Hg_2Cl_2 (in the unit of Pascal) can be evaluated from the

$$p_A = e^{(a - b/T)}, \tag{8}$$

following formula as a function of temperature: in which a = 29.75, b = 11767.1.

3. Results and Discussion

The six dimensionless parameters, namely Gr, Ar, Pr, Le, C_v Pe, and thermo-physical properties for the operating conditions of this study are considered in this study. Because the molecular weight of a noble element (Kr) is not equal to that of the crystal component (Hg_2Cl_2) during the physical vapor transport, both solutal and/or thermal effects should be considered in this study.

Fig. 2 shows the interfacial distributions of total molar flux (moles $cm^{-2}s^{-1}$) of Hg_2Cl_2 for two gravity accelerations ($1g_0$, $0.1g_0$, where $1g_0 = 981$ cm s^{-2}), based on ΔT = 90 K (350°C → 260°C), P_B = 20 Torr, Ar = 5.0, Pr = 0.8, Le = 0.95, $Gr_t = 2.9 \times 10^4$, $Gr_s = 2.6 \times 10^6$, Pe = 4.5, C_v = 1.01. The horizontal orientations and the linear temperature profiles at walls are considered in this case. Here,

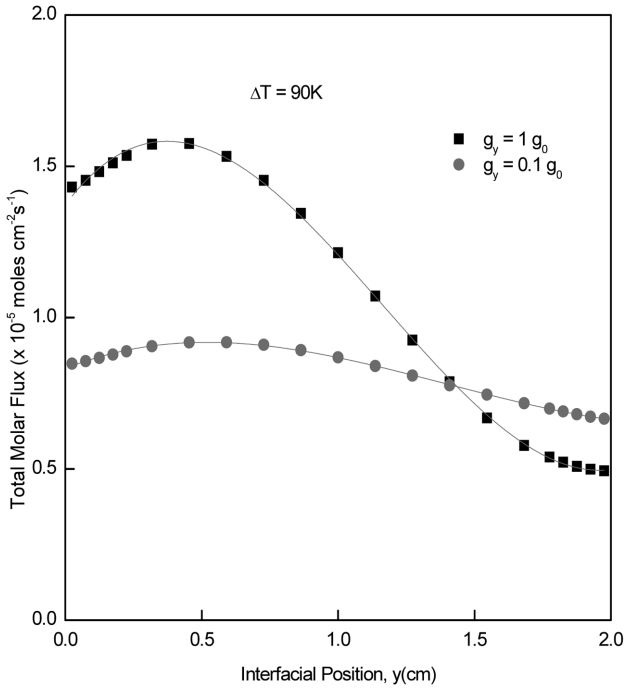

Fig. 2. Interfacial distributions of total molar flux (moles $cm^{-2}s^{-1}$) of Hg_2Cl_2 for two gravity accelerations ($1g_0$, $0.1g_0$, where $1g_0$ = 981 cm s^{-2}), based on ΔT = 90 K ($350^oC \rightarrow 260_oC$), P_B = 20 Torr, Ar = 5.0, Pr = 0.8, Le = 0.95, $Gr_t = 2.9 \times 10^4$, $Gr_s = 2.6 \times 10^5$, Pe = 4.5, C_v = 1.01.

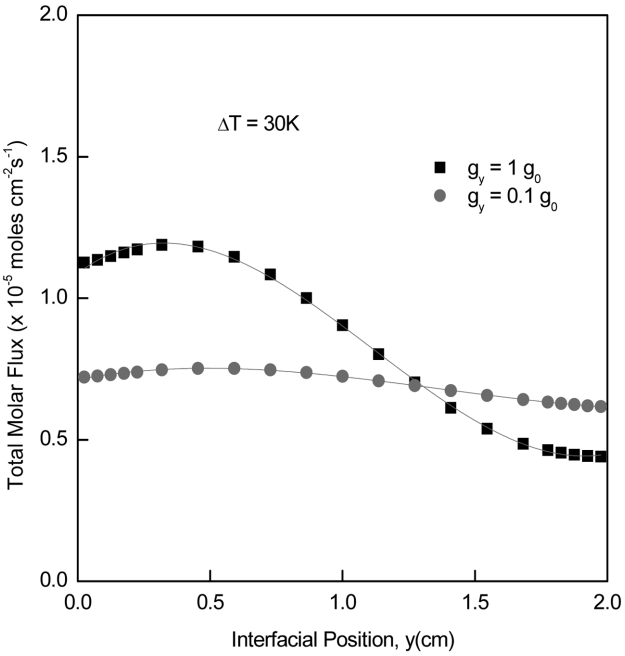

Fig. 3. Interfacial distributions of total molar flux (moles $cm^{-2}s^{-1}$) of Hg_2Cl_2 for two gravity accelerations ($1g_0$, $0.1g_0$, where $1g_0$ = 981 cm s^{-2}), based on ΔT = 30 K ($350^oC \rightarrow 320_oC$), P_B = 20 Torr, Ar = 5.0, Pr = 0.8, Le = 0.45, $Gr_t = 3.9 \times 10^4$, $Gr_s = 5.4 \times 10^5$, Pe = 3.2, C_v = 1.04.

the subscript of 0 denotes the normal gravity acceleration of 981 cm•s^{-2}. With decreasing the gravitational acceleration from 1 g_0 down to 0.1 g_0, the total molar flux for 0.1 g_0 is reduced by a factor of 0.57, in comparison with 1 g_0. As depicted in Fig. 2, similar to the earlier results of Markham, Greenwell and Rosenberger [2], one sees that the convective flow can cause significant non-uniformities in the total molar flux, with the specific distribution revealing dominance of solutal convection. Even though not shown here, the single convection cell flows towards the growing interface in the lower half of the growth ampoule, thus better supplying this part of the interface with vapor supersaturated in component A. Note that if there is thermal convection alone, with the left part of the ampoule warmer than the right part, an oppositely rotating roll would appear and, thus, result in enhancing the growth of crystal in the upper half of the interface [2]. As shown in Fig. 2, the interfacial distributions of total molar flux shows asymmetrical with respect to y = 1.0 cm, which indicates the presence of asymmetrical convection. Therefore, the asymmetrical convection cell in front of the crystal interface indicates three dimensional flow structures. It is also obvious that from the point of view of the uniformity, the total molar flux along the interfacial positions at $g_y = 0.1\ g_0$ exhibits to have a relatively flat structure compared to that at $g_y = 1\ g_0$. It indicates a factor of ten reduction in the gravitational level is enough to suppress convective effects on the crystal growth flux.

Fig. 3 shows interfacial distributions of total molar flux (moles $cm^{-2}s^{-1}$) of Hg_2Cl_2 for two gravity accelerations ($1g_0$, $0.1g_0$, where $1g_0$ = 981 cm s^{-2}), based on ΔT = 30 K ($350^oC \rightarrow 320^oC$), P_B = 20 Torr, Ar = 5.0, Pr = 0.8, Le = 0.45, $Gr_t = 3.9 \times 10^4$, $Gr_s = 5.4 \times 10^5$, Pe = 3.2, C_v = 1.04.

In PVT processes, the temperature difference between source and crystal is one of the major parameters as well as a driving force for the mass transport. Under otherwise unchanged process conditions, decreasing the temperature difference for Ar = 5 gives similar results to Fig. 2. This suggests that in a $0.1g_0$ of gravity environment the total molar fluxes would be increased by using smaller aspect ratio ampoules (Fig. 4) or larger temperature differences between source and crystal (Fig. 2), without the drawback of increased convection that would result from these measures on ground experiments. Compared with Figs. 2 and 3, it is clear that the effects of thermally buoyancy driven convection are important even in reduced gravity environments. The maximum total molar flux at ΔT = 90 K reaches at 1.57 moles $cm^{-2}s^{-1}$, and the maximum flux of 1.18 moles $cm^{-2}s^{-1}$ is obtained at ΔT = 30 K. When the temperature difference is de-

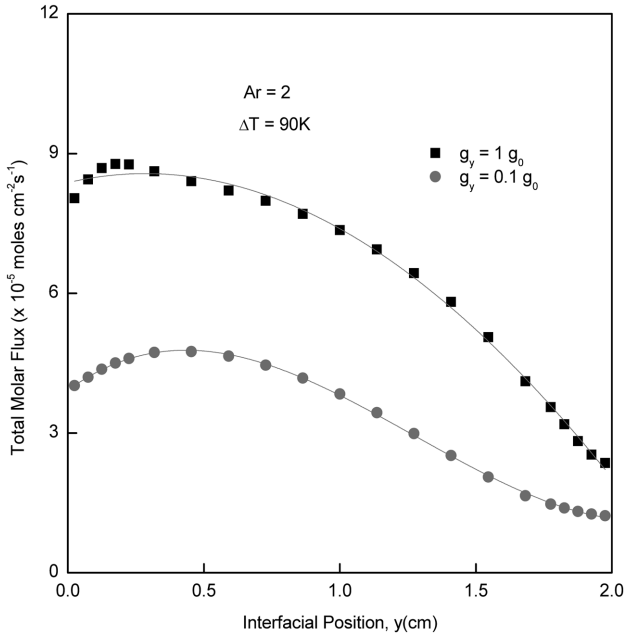

Fig. 4. Interfacial distributions of total molar flux (moles $cm^{-2}s^{-1}$) of Hg_2Cl_2 for two gravity accelerations ($1g_0$, $0.1g_0$, where $1g_0$ = 981 cm s^{-2}), based on ΔT = 90 K ($350^oC \rightarrow 260^oC$), P_B = 20 Torr, Ar = 2.0, Pr = 0.8, Le = 0.95, $Gr_t = 2.9 \times 10^4$, $Gr_s = 2.6 \times 10^5$, Pe = 4.5, C_v = 1.01.

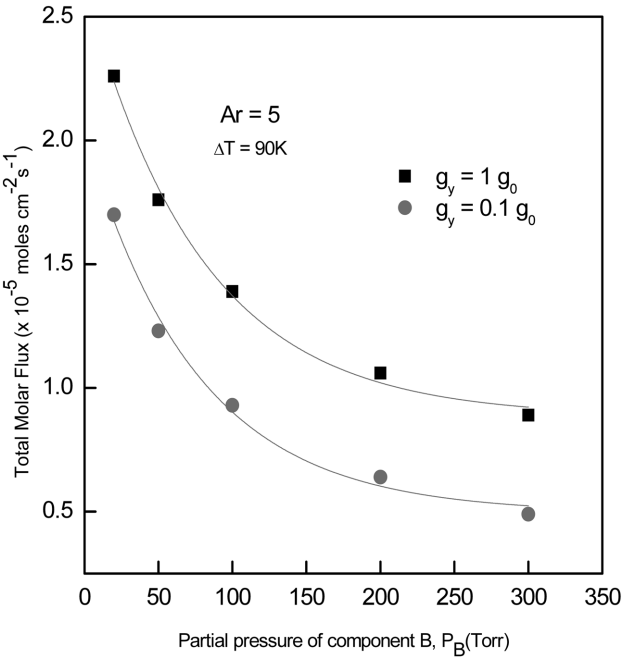

Fig. 5. Effects of partial pressure of component B, P_B (Torr) on the total molar flux of Hg_2Cl_2 in terms of moles $cm^{-2}s^{-1}$ for various partial pressures of component B, P_B (Torr), $20 \le P_B \le 300$, based on ΔT = 90 K ($350^oC \rightarrow 260^oC$), Ar = 5.

creased from 350^oC by a factor of 0.33, the corresponding maximum molar flux is also decreased from 1.57 moles $cm^{-2}s^{-1}$ by a factor of 0.75.

Fig. 4 shows interfacial distributions of total molar flux (moles $cm^{-2}s^{-1}$) of Hg_2Cl_2 for two gravity accelerations ($1g_0$, $0.1g_0$, where $1g_0$ = 981 cm s^{-2}), under the same conditions except for Ar = 2 as Fig. 2. The temperature difference between source and crystal remain unchanged and the source temperature of 350^oC is fixed so that the effects of thermo-physical properties due to the variations in temperature could be negligible. Note that in actual crystal experiments of Hg_2Cl_2, the typical source and crystal temperature correspond to 320^oC and 290^oC, respectively. It is interesting that the maximum total molar fluxes appear near the bottom of the ampoule with decreasing the aspect ratio (transport length-to-width) from Ar = 5 down to 2. In other words, the width is increased from y = 2 cm to 5 cm. As shown in Fig. 2, the maximum total molar fluxes occur near at the y = 0.5 cm for gravity accelerations under consideration in this study. Fig. 4 shows the total molar flux decreases linearly in accordance with interfacial position. In addition, the maximum total molar flux for normal gravity level is greater than that for $0.1g_0$ by a factor of 2. But, the total molar flux is likely to converge to some flux close to 0.55. This suggests the effect of side wall suppresses the convective flow and is greater for normal gravity level than the level of gravity acceleration with a factor of ten reduction.

Greenwell et al. [1] showed that small non-uniformities in growth rates can occur even in the absence of gravity and are associated with the recirculation of the inert gas. This was also true in numerical calculations as can be seen in Figs. 2 through 5. Even for situations of purely diffusive transport the growth rate was not strictly uniform, with growth being greater near the center than the edges. However, theses growth rate variations were very small and within tolerable limits, unlike the large variations resulting from convective contributions.

Fig. 5 shows effects of partial pressure of component B, P_B (Torr) on the total molar flux of Hg_2Cl_2 in terms of moles $cm^{-2}s^{-1}$ for various partial pressures of component B, P_B (Torr), $20 \le P_B \le 300$, for the horizontal orientations and the temperature difference (ΔT = 90 K) between the source and the crystal region of $320^oC \rightarrow 290^oC$, Ar = 5, L = 10 cm, with the linear temperature profiles at walls. As plotted in Fig. 5, the total molar fluxes decay first order exponentially with the partial pressure of component B, P_B (Torr) for 20 Torr $\le P_B \le$ 300 Torr, and two gravity accelerations of $g_y = 1g_0$ and $0.1g_0$. For the range of 20 Torr $\le P_B \le$ 100 Torr, the molar fluxes drop significantly, and, for 100 Torr $\le P_B \le$ 300 Torr, decreases slowly. In other words, the total molar fluxes decrease sharply near P_B = 20 Torr, and, then since

P_B = 100 Torr, decrease slowly until at P_B = 300 Torr. At both $g_y = 1g_0$ and $0.1g_0$, the decrease in the total molar flux appears relatively small for 200 Torr ≤ P_B ≤ 300 Torr, and the corresponding regression profile is nearly flat. Moreover, as the P_B is increased from 20 Torr to 300 Torr, i.e. by a factor of 15, and the total molar flux for $g_y = 1g_0$ is decreased from 2.26×10^{-5} down to 0.89×10^{-5} moles $cm^{-2}s^{-1}$ by a factor of 0.39, and for $g_y = 0.1g_0$, from 1.7×10^{-5} to 0.49×10^{-5} moles $cm^{-2}s^{-1}$ by a factor of 0.29, respectively. Consequently, with decreasing the gravitational acceleration from $1g_0$ down to $0.1g_0$, the factor of reduction in molar flux is 0.74, which reflects reduction in the effects of convection. Moreover, the gaps between the total molar flux for $g_y = 1g_0$ and $0.1g_0$ is smaller for the range of 20 Torr ≤ P_B ≤ 50 Torr, and then, become larger 50 Torr ≤ P_B ≤ 100 Torr and, for the range of P_B more than 100 Torr, appears invariant. The effect of gravity acceleration is likely to affect in the main the total molar flux rather than the effect of a convective parameter of partial pressure of component B, P_B.

Fig. 6 shows the interfacial distributions of total molar flux (moles $cm^{-2}s^{-1}$) of Hg_2Cl_2 for two gravity accelerations ($1g_0$, $0.1g_0$, where $1g_0 = 981$ cm s^{-2}), based on ΔT = 90 K (350°C → 260°C), P_B = 300 Torr, Ar = 5. The operation parameters for $g_y = 1g_0$ in Fig. 5 are as follows: Ar = .0, Pr = 0.75, Le = 1.28, $Gr_t = 5.2 \times 10^4$, $Gr_s = 3.8 \times 10^5$, Pe = .9, C_v = 1.1. As shown in Fig. 6, like the cases of P_B = 20 Torr, i.e., as shown in Fig. 2, the maximum molar flux for two gravitational accelerations appear at the neighborhood of y = 0.5 cm, and the molar fluxes versus the interfacial positions show asymmetrical against the position of y = 1.0 cm. The molar fluxes for two different gravities of 1 and $0.1g_0$ converge at the neighborhood of 0.2, while for the cases of P_B = 20 Torr, the molar fluxes approach the value of 0.8×10^{-5} moles $cm^{-2}s^{-1}$ near at y = 2.0 cm. This result indicates that the convection for P_B = 20 Torr is likely to be more predominant near at y = 2.0 cm than for P_B = 200 Torr. In comparisons of Figs. 2 and 6, an increase in the partial pressure of component B, P_B from 20 to 200 Torr suppresses the convective effects. The maximum molar flux for P_B = 20 Torr and $1g_0$ is greater than for P_B = 200 by a factor of 2.45, while for the gravity level of $0.1g_0$ in Fig. 6, the maximum molar flux for P_B = 20 Torr is greater than for P_B = 200 Torr by a factor of 3.54. Also, the difference between the maximum and the minimum molar flux for P_B = 20 Torr and $1g_0$ is greater than for P_B = 200 Torr by a factor of 2.2, which implies the mass transport by the diffusion is strong to enough to cause more significant non-uniformities with increasing the partial pressure of component B, P_B.

Fig. 7 shows the total molar flux of Hg_2Cl_2 in terms of moles $cm^{-2}s^{-1}$ as a function of gravity accelerations, $10^{-4}\ g_0 \le g_y \le 1g_0$, based on P_B = 200 Torr and ΔT = 90 K.

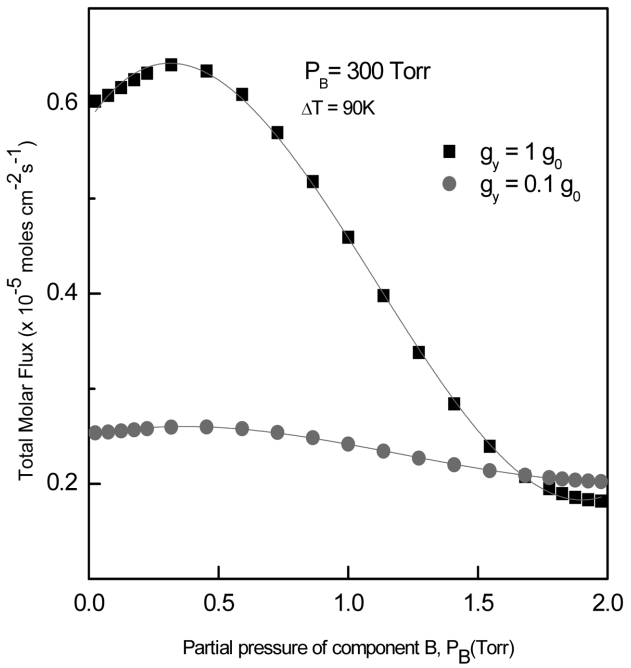

Fig. 6. Interfacial distributions of total molar flux (moles $cm^{-2}s^{-1}$) of Hg_2Cl_2 for two gravity accelerations ($1g_0$, $0.1g_0$, where $1g_0$ = 981 cm s^{-2}), based on ΔT = 90 K (350°C → 260°C), P_B = 300 Torr, Ar = 5.

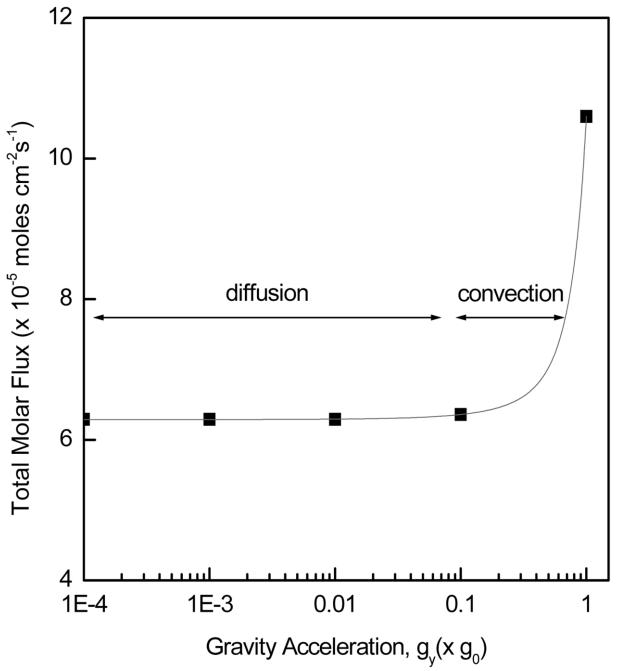

Fig. 7. The total molar flux of Hg_2Cl_2 in terms of moles $cm^{-2}s^{-1}$ as a function of gravity accelerations, $10^{-4}\ g_0 \le g_y \le 1g_0$, based on P_B = 200 Torr and ΔT = 90 K.

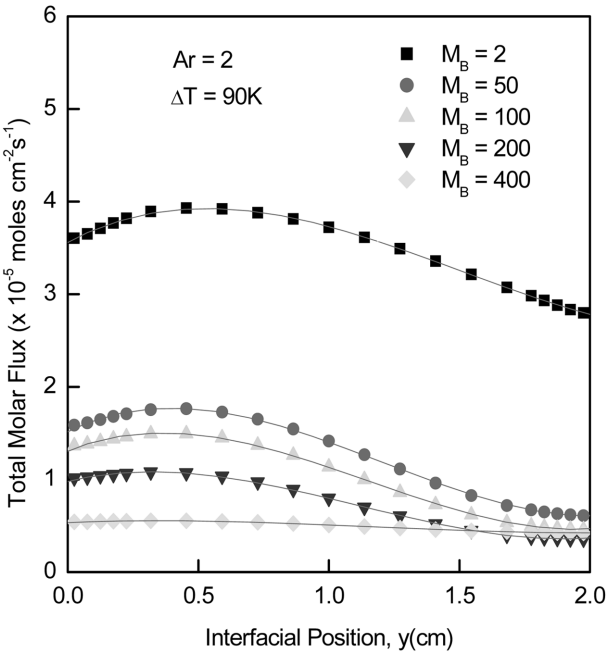

Fig. 8. Interfacial distributions of total molar flux (moles $cm^{-2}s^{-1}$) of Hg_2Cl_2 for various molecular weight of component B, M_B, $2 \le M_B \le 400$, based on Ar = 5 Torr and ΔT = 90 K.

The convection mode is predominant over the diffusion mode for 10^{-1} $g_0 \le g_y \le 1g_0$. The convection mode is transited into the diffusion mode at $g_y = 0.1g_0$. And, down to $g_y = 10^{-4}$ g_0, the diffusion becomes predominant. As seen in Fig. 7, the total molar fluxes drop sharply for 10^{-1} $g_0 \le g_y \le 1g_0$. This indicates the mass transport is diffusion-dominated under the microgravity environments less than $0.1g_0$. One can see that the effect of thermo-solutal convection is first important and then decreases rapidly and eventually the mode of transport becomes largely diffusion.

Fig. 8 shows the interfacial distributions of total molar flux (moles $cm^{-2}s^{-1}$) of Hg_2Cl_2 for various molecular weight of component B, M_B, $2 \le M_B \le 400$, based on Ar = 5 Torr and ΔT = 90 K. One also investigated situations when thermal convection might dominate solutal convection. This could occur when an inert gas having a molecular weight M_B closer to that of the crystallizing material is used. The results of varying molecular weight of component B, M_B in a horizontal system with Ar = 5 and the larger temperature difference are shown in Fig. 8. As the molecular weight of B is increased from 2 up to 400, one can see that the effect of solutal convection decreases rapidly for $2 \le M_B \le 50$, and, for $50 \le M_B \le 400$, eventually the transport becomes largely diffusive. For conditions under consideration, Note that only when the molecular weights of A and B are equal does the thermal density gradient overcome the solutal gradient. It is concluded that unless the two components have molecular weights very close to each other, the dominant mode of convection is likely to be solutal. It is emphasized that the effects of solutal convection are reflected through the density gradient and binary diffusivity coefficient. The maximum total molar fluxes occur in the neighborhood of y = 0.5 cm.

4. Conclusions

The convection transport in crystal growth of Hg_2Cl_2-Kr during the physical vapor transport appears to be predominant over the diffusive transport. Thus, for vapor growth near normal gravity acceleration levels less than $0.1g_0$ would be needed to suppress convection. Even under microgravity environments of $0.1g_0$, i.e., for the diffusion mode, the nonouniformites in front of the crystal regions appear. For the levels of gravitational acceleration from more than $0.1g_0$ up to $1g_0$, there are appropriate to ensure the mass transport by the means of diffusive-convection. The asymmetrical convection cell in front of the crystal interface indicates three dimensional flow structures. It is also obvious that from the point of view of the uniformity, the total molar flux along the interfacial positions at $g_y = 0.1g_0$ exhibits to have a relatively flat structure compared to that at $g_y = 1g_0$. For $2 \le M_B \le 50$, it is concluded that unless the two components have molecular weights very close to each other, the dominant mode of convection is likely to be solutal. For gravity accelerations less than 1.0×10^{-4} g_0, the total molar fluxes are nearly invariant for ΔT = 90 K and Ar = 5. For the range of 20 Torr $\le P_B \le$ 100 Torr, the molar fluxes drop significantly, and, for 100 Torr $\le P_B \le$ 300 Torr, decreases slowly. The total molar fluxes decay first order exponentially with the partial pressure of component B, P_B (Torr) for 20 Torr $\le P_B \le$ 300 Torr, and two gravity accelerations of $g_y = 1g_0$ and $0.1g_0$.

Acknowledgement

This work was financially supported by the Hannam University under Grant No. 2012A021 (April 1, 2012 through March 31, 2013).

References

[1] D.W. Greenwell, B.L. Markham and F. Rosenberger,

"Numerical modeling of diffusive physical vapor transport in cylindrical ampoules", J. Crystal Growth 51 (1981) 413.
[2] B.L. Markham, D.W. Greenwell and F. Rosenberger, "Numerical modeling of diffusive-convective physical vapor transport in cylindrical vertical ampoules", J. Crystal Growth 51 (1981) 426.
[3] B.S. Jhaveri and F. Rosenberger, "Expansive convection in vapor transport across horizontal enclosures", J. Crystal Growth 57 (1982) 57.
[4] B.L. Markham and F. Rosenberger, "Diffusive-convective vapor transport across horizontal and inclined rectangular enclosures", J. Crystal Growth 67 (1984) 241.
[5] A. Nadarajah, F. Rosenberger and J. Alexander, "Effects of buoyancy-driven flow and thermal boundary conditions on physical vapor transport", J. Crystal Growth 118 (1992) 49.
[6] F. Rosenberger, J. Ouazzani, I. Viohl and N. Buchan, "Physical vapor transport revised", J. Crystal Growth 171 (1997) 270.
[7] H. Zhou, A. Zebib, S. Trivedi and W.M.B. Duval, "Physical vapor transport of zinc-telluride by dissociative sublimation", J. Crystal Growth 167 (1996) 534.
[8] W.M.B. Duval, "Convection in the physical vapor transport process--I: Thermal convection", J. Chem. Vapor Deposition 2 (1994a) 188.
[9] W.M.B. Duval, "Convection in the physical vapor transport process--II: Thermosolutal convection", J. Chem. Vapor Deposition 2 (1994b) 282.
[10] W.M.B. Duval, "Transition to chaos in the physical vapor transport process--I: fluid mechanics problem phenomena in microgravity", Fluids Eng. Div. ASME 175 (1993) 51.
[11] W.M.B. Duval, N.E. Glicksman and B. Singh, "Physical vapor transport of mercurous chloride crystals; design of a microgravity experiment", J. Crystal Growth 174 (1997) 120.
[12] P.A. Tebbe, S.K. Loyalka and W.M.B. Duval, "Finite element modeling of asymmetric and transient flow fields during physical vapor transport", Finite Elements in Analysis and Design 40 (2004) 1499.
[13] G.T. Kim, W.M.B. Duval, N.B. Singh and M.E. Glicksman "Thermal convective effects on physical vapor transport growth of mercurous chloride crystals (Hg_2C1_2) for axisymmetric 2-D cylindrical enclosure", Modelling. Simul. Mater. Sci. Eng. 3 (1995) 331.
[14] G.T. Kim, W.M.B. Duval and M.E. Glicksman "Thermal convection in physical vapour transport of mercurous chloride (Hg_2Cl_2) for rectangular enclosures", Modelling. Simul. Mater. Sci. Eng. 5 (1997) 289.
[15] G.T. Kim, W.M.B. Duval and M.E. Glicksman "Effects of asymmetric temperature profiles on thermal convection during physical vapor transport of Hg_2Cl_2", Chem. Eng. Comm. 162 (1997) 45.
[16] G.-T. Kim and K.-H. Lee, "Parametric studies on convection during the physical vapor transport of mercurous chloride (Hg_2Cl_2)", J. Korean Crystal Growth and Crystal Technology 14 (2004) 281.
[17] G.T. Kim, "Convective-diffusive transport in mercurous chloride (Hg_2Cl_2) crystal growth", J. Ceramic Processing Research 6 (2005) 110.
[18] S.J. Yosim and S.W. Mayer, "The mercury-mercuric chloride system", J. Phys. Chem. 60 (1960) 909.
[19] N.B. Singh, M. Gottlieb, A.P. Goutzoulis, R.H. Hopkins and R. Mazelsky, "Mercurous bromide acousto-optic devices", J. Crystal Growth 89 (1988) 527.
[20] F. Rosenberger and G. Müller, "Interfacial transport in crystal growth, a parameter comparison of convective effects", J. Crystal Growth 65 (1983) 91.
[21] S.V. Patankar, "Numerical heat transfer and fluid flow" (Hemisphere Publishing Corp., Washington D.C., 1980).